

*Supplement of*

**Formation and characteristics of secondary aerosols in an industrialized environment during cold seasons**

Yangzhou Wu<sup>1</sup>, Xinlei Ge<sup>1</sup>, Junfeng Wang<sup>1</sup>, Yafei Shen<sup>1</sup>, Zhaolian Ye<sup>2</sup>, Shun Ge<sup>3</sup>,  
Yun Wu<sup>1</sup>, Huan Yu<sup>1</sup>, Mindong Chen<sup>1</sup>

<sup>1</sup>Jiangsu Key Laboratory of Atmospheric Environment Monitoring and Pollution Control, Collaborative Innovation Center of Atmospheric Environment and Equipment Technology, School of Environmental Sciences and Engineering, Nanjing University of Information Science and Technology, Nanjing 210044, China

<sup>2</sup>College of Chemistry and Environmental Engineering, Jiangsu University of Technology, Changzhou 213001, China

<sup>3</sup>Nanjing Tianbo Environmental Technology Co., Ltd, Nanjing 210047, China

*Correspondence to:* Xinlei Ge ([caxinra@163.com](mailto:caxinra@163.com)) and Mindong Chen ([chenmdnuist@163.com](mailto:chenmdnuist@163.com))

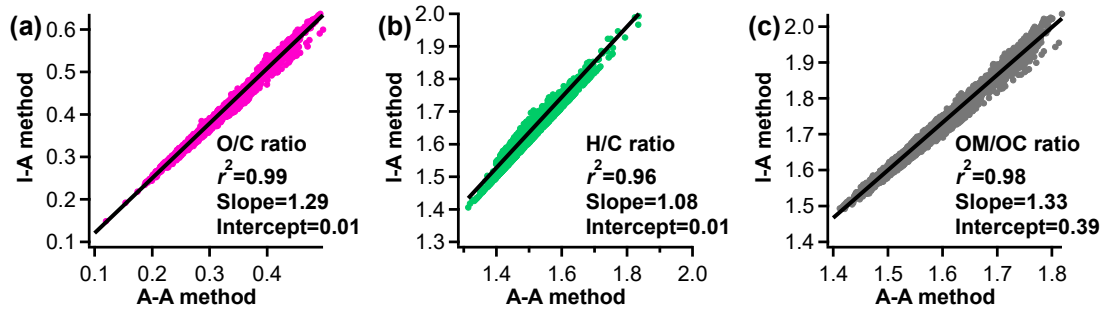


Figure S1. Scatter plots of the O/C ratios (a), H/C ratios (b), and OM/OC ratios (c) calculated by using the I-A method versus those by using the A-A method.

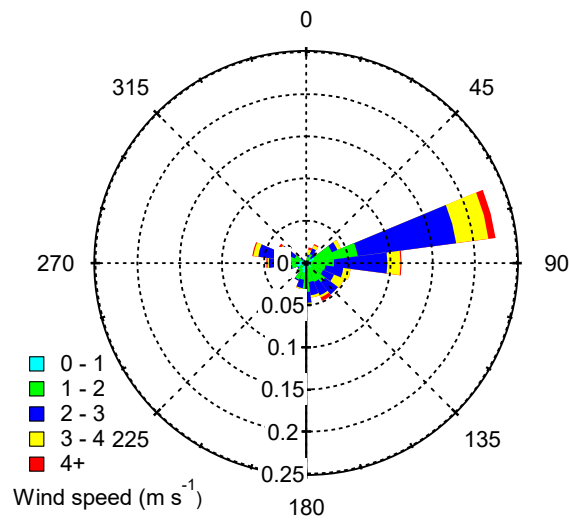


Figure S2. The wind rose plot for the entire campaign (a similar plot has been presented in the supplement of our previous work (Wang et al., 2016)).

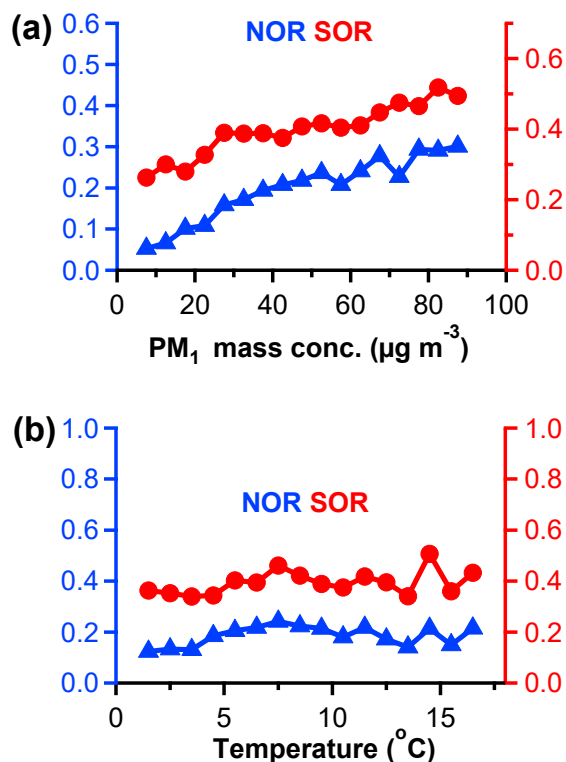


Figure S3. (a) Variations of nitrogen oxidation ratio (NOR) and sulfur oxidation ratio (SOR) against PM<sub>1</sub> concentrations (a) and temperatures (b).

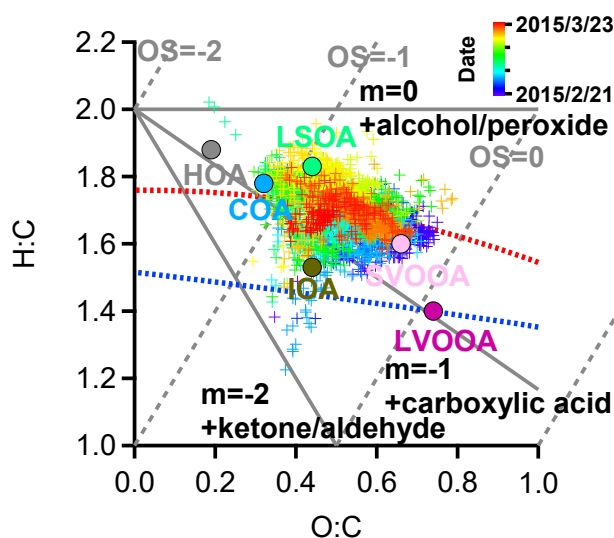


Figure S4. Van Krevelen diagram of H:C vs. O:C ratios for all OA data colored by time, the blue and red dashed lines correspond to the right and left gray dashed lines in the  $f_{44}$  vs.  $f_{43}$  triangle plot of Fig. 7b; the grey lines represent the addition of a particular functional group to an aliphatic carbon (Heald et al., 2010).

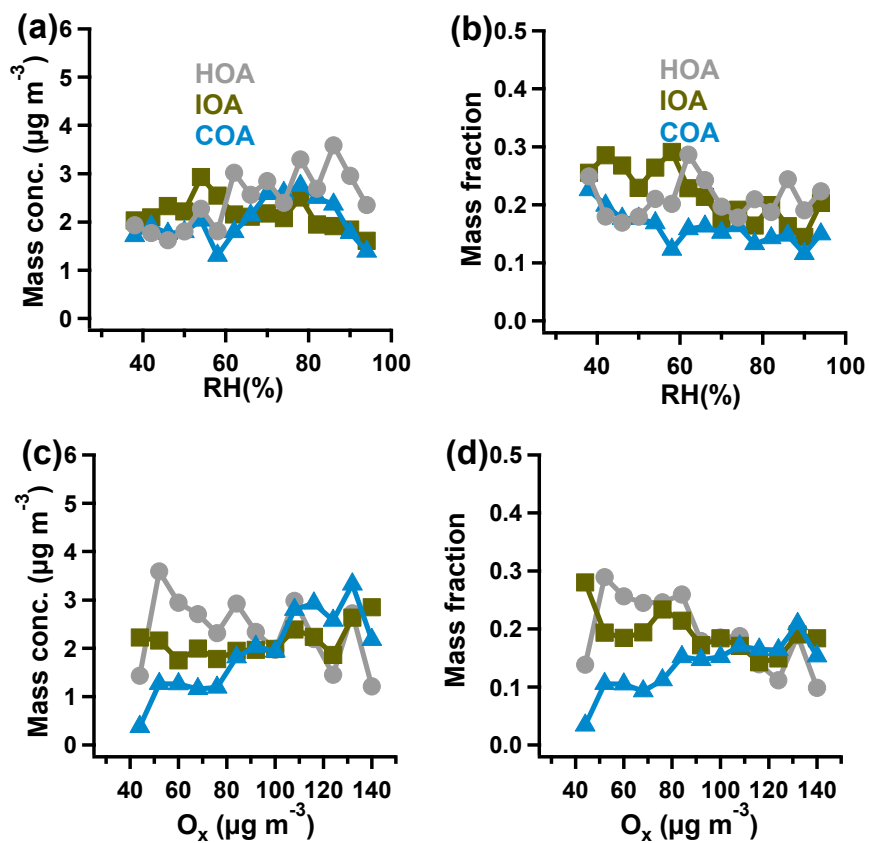


Figure S5. Mass concentrations (a) and fractional contributions (b) of the HOA, IOA and COA as a function of RH (5% increment); mass concentrations (c) and fractional contributions of the HOA, IOA and COA as a function of  $\text{O}_x$  concentrations (8  $\mu\text{g}/\text{m}^3$  increment).

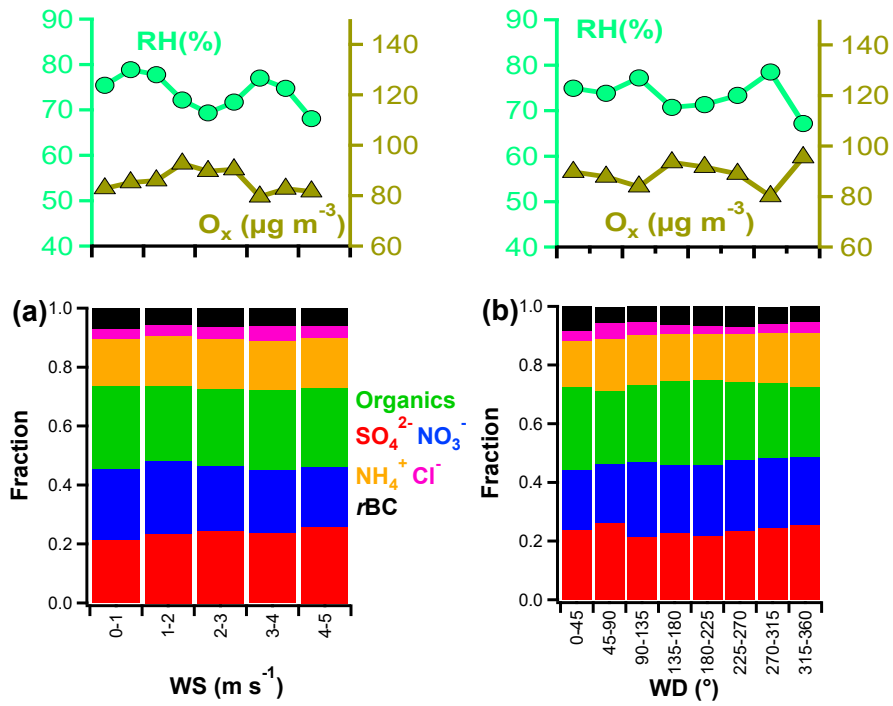


Figure S6. Mass fractions of the six PM<sub>1</sub> components, and corresponding average RH values and O<sub>x</sub> concentrations at different wind speeds (1 m/s increment) (a), and wind directions (45° increment).

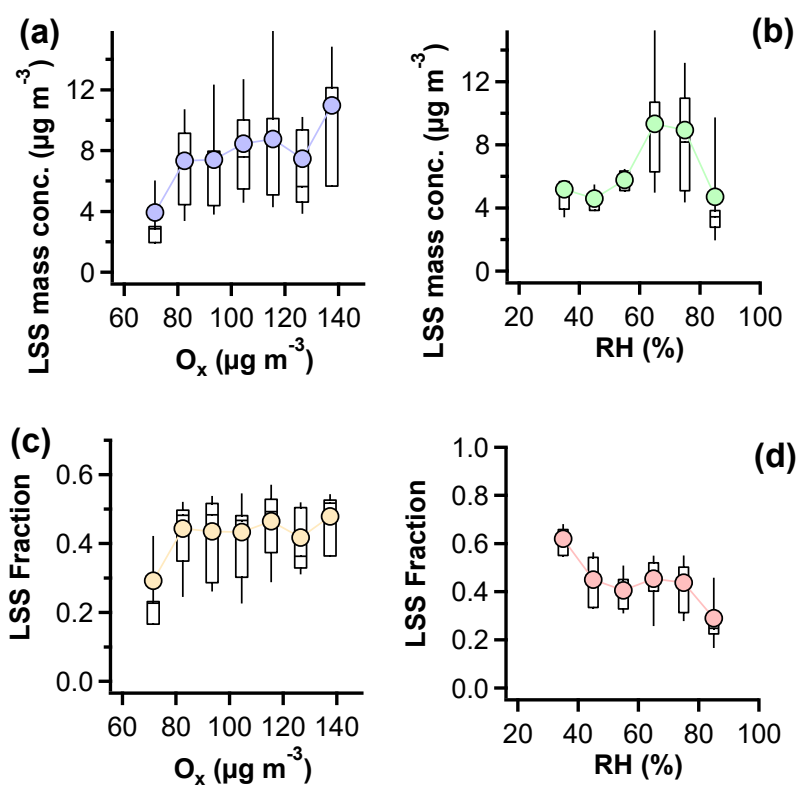


Figure S7. Mass concentrations (a) and fractional contributions (c) of LSS concentrations (the sum of LSOA and SVOOA concentrations) against  $\text{O}_x$  concentrations ( $10 \mu\text{g}/\text{m}^3$  increment); Mass concentrations (b) and fractional contributions (d) of LSS concentrations against RH ( $10\%$  increment)(the lines and solid triangles are the mean values, the lines in the boxes are the median values, the upper and lower boundaries of the boxes indicate the 75th and 25th percentiles, and the whiskers above and below the boxes indicate the 90th and 10th percentiles).

References:

Heald, C. L., Kroll, J. H., Jimenez, J. L., Docherty, K. S., DeCarlo, P. F., Aiken, A. C., Chen, Q., Martin, S. T., Farmer, D. K., and Artaxo, P.: A simplified description of the evolution of organic aerosol composition in the atmosphere, *Geophys. Res. Lett.*, 37, L08803, 10.1029/2010gl042737, 2010.

Wang, J., Onasch, T. B., Ge, X., Collier, S., Zhang, Q., Sun, Y., Yu, H., Chen, M., Prévôt, A. S. H., and Worsnop, D. R.: Observation of fullerene soot in eastern China, *Environ. Sci. Technol. Lett.*, 3, 121-126, 10.1021/acs.estlett.6b00044, 2016.